Size dependent bending and vibration analysis of functionally graded micro beams based on modified couple stress theory and neutral surface position

Abdelouahed Tounsi, K.S. Al-Basyouni, S.R. Mahmoud

PII: S0263-8223(15)00002-1
DOI: http://dx.doi.org/10.1016/j.compstruct.2014.12.070
Reference: COST 6130

To appear in: *Composite Structures*

Size dependent bending and vibration analysis of functionally graded micro beams based on modified couple stress theory and neutral surface position

Abdelouahed Tounsi[3], K.S.Al-Basyouni[1] and S. R. Mahmoud[1, 2]

(1) Department of Mathematics, Faculty of Science, King Abdulaziz University, Saudi Arabia.

(2) Mathematics Department, Faculty of Science, University of Sohag, Egypt.

(3) Material and Hydrology Laboratory, University of Sidi Bel Abbes, Faculty of Technology, Civil Engineering Department, Algeria.

kalbasyouni@kau.edu.sa , tou_abdel@yahoo.com ; srhassan@kau.edu.sa

Abstract

In this project, a novel unified beam formulation and a modified couple stress theory (MCST) that considers a variable length scale parameter in conjunction with the neutral axis concept are proposed to study bending and dynamic behaviors of functionally graded (FG) micro beam. New first and sinusoidal beam theories together with the classical beam theory can easily formulated from this approach. The Mori–Tanaka homogenization technique is used to predict all effective material properties of the FG micro beams – including the length scale parameter – which are assumed to vary in the thickness direction. The constructed models include the physical length scale parameter which can introduce the size effect. Some results are presented to show the effects of the material length scale parameter, the power law index, and shear deformation on the bending and dynamic behaviors of FG micro beams.

***Keywords**:* Resins; Vibration; Micro-mechanics; Analytical modeling; Modified couple stress theory

1. Introduction

Functionally graded materials (FGMs) are widely used in a variety of industries due to their important physical properties that vary as a power-law distribution, continuously as a function of position along certain dimensions. Such materials were included to gain benefits of the desired physical properties of each constituent material without interface problems.

In view of the increasing interest in using FGMs in the modern technology, such materials have been widely used recently in micro/nanoelectromechanical systems (MEMS/NEMS), such as the components in the form of shape memory alloy thin films with a global thickness in micro- or nano-scale [1–3], electrically actuated MEMS devices [4–6], and atomic force microscopes (AFMs) [7]. Furthermore, the practical investigations demonstrate as the thickness of the structures becomes on the magnitude of microns and sub-microns, the size effect of material plays a great role in mechanical responses of such structures [8, 9]. Consequently, the classical continuum theories are unsuitable to analyze the behavior of micro-scale structures and the use of size-dependent theories (i.e., strain gradient elasticity and couple stress theories) having internal material length scale parameters is necessary. However, since the classical couple stress theory introduces two separate material length scale parameters [8, 9]; a great problem is found to experimentally asses the micro-structural material length scale parameters. Because of the encountered problems in assessing the micro-structural material length scale parameters, Yang et al. [10] developed a modified couple stress model, which could investigate micro systems with only one material length scale parameter. The modified couple stress model has been employed widely nowadays. Park and Gao [11] investigated Euler-Bernoulli beams, by employing the mentioned model. Kong et al. [12] analyzed also the size-dependent natural frequency of these beams. Furthermore, Ma et al. [13, 14] have illustrated size-dependent Timoshenko and Reddy- Levinson beam models based on modified couple stress theory.

Recently, study of micro-scale functionally graded (FG) beams, by employing modified couple stress model, has attracted several researchers. Asghari et al. [15, 16] studied the bending and dynamic responses of FG Euler-Bernoulli and Timoshenko beam theories neglecting Poisson's effect. Ke and Wang [17] analyzed size effect on dynamic stability of FG micro beams. Using different beam theories, Nateghi et al. [18] investigated size-dependant buckling behavior of FG micro beams. Reddy [19] studied size-dependant nonlinear response of FG micro beams. However, in all works on FG micro-beams mentioned above, the length scale parameters employed in the formulation are considered as constants. The only work in the open literature that takes into consideration the variations in the length scale parameters seems to be that by Kahrobaiyan et al. [20]. In this paper, the authors present a formulation based on the strain gradient elasticity theory in conjunction with the Euler-Bernoulli beam model. However, Euler-Bernoulli model neglects the shear deformation effect and consequently it underestimates deflections and overestimates the natural frequencies in case of thick beams where shear deformation effects are significant.

In this work, a new modified couple stress theory is developed to study the bending and vibration responses of FG micro-beams having a variable length scale parameter on the basis on a unified beam formulation in conjunction with the neutral axis concept. Contrary to the other high order beam theories, the transverse displacement in this formulation is assumed to consist of bending and shear components. As a result, a new first beam theory (NFBT) and a new sinusoidal beam theory (NSBT) together with the classical beam theory (CBT) are easily created. In addition, this micro-scale beam model introduces the material length scale parameter which can capture the size effect. The material properties of the FG micro-scale beams including the length scale parameter are assumed to vary in the thickness direction and are assessed through the Mori–Tanaka homogenization technique and the classical rule of mixture. Since, the material properties of FG micro-scale beam vary through the thickness direction; the neutral axis of such micro-scale beam may not coincide with its geometric middle plane [21 – 26]. In addition, Bouremana et al [22] and Yahoobi and Feraidoon [21] show that the stretching – bending coupling in the constitutive equations of an FG beam does not exist when the coordinate system is located at the physical neutral axis of the beam. The governing equations and the related boundary conditions are deduced by employing the Hamilton's principle. The effects the material length scale parameter, different material compositions, shear deformation on the bending and free vibration response of FG micro-scale beams are investigated in this work. The present results are also compared with previously published results to establish the validity of the present formulation.

2 Theoretical formulations

In this work a FG micro-scale beam of length L, width b, and thickness h is considered. The Cartesian coordinate system, (x, z), with the origin at the left end of the micro-scale beam is employed in this study. The x axis is chosen to be the undeformed centroidal axis of the beam and the z axis is perpendicular to the x axis. Due to asymmetry of material properties of FG beams with respect to median axis, the stretching and bending equations are coupled. But, if the origin of the coordinate system is suitably selected in the thickness direction of the FG micro-scale beam so as to be the neutral axis, the properties of the FG micro-scale beam being symmetric with respect to it. To specify the position of neutral axis of FG micro-scale beams, two different axis are considered for the measurement of z, namely, z_{ms} and z_{ns} measured from the centroidal axis and the neutral axis of the micro-scale beam, respectively, as depicted in Figure 1.

The volume-fraction of ceramic V_C is expressed based on z_{ms} and z_{ns} coordinates as

$$V_C = \left(\frac{z_{ms}}{h} + \frac{1}{2}\right)^k = \left(\frac{z_{ns} + z_0}{h} + \frac{1}{2}\right)^k, \quad k \geq 0 \tag{1}$$

where k in Eq. (1) is the volume fraction exponent, also referred to as the gradient index and z_0 is the distance of neutral axis from the centroidal axis. According to Mori–Tanaka homogenization scheme, the effective Bulk Modulus (K) and the effective shear modulus (G) are given by [27 – 29]:

$$\frac{K - K_m}{K_C - K_m} = \frac{V_C}{1 + (1 - V_C)\dfrac{3(K_C - K_m)}{3K_m + 4G_m}} \tag{2a}$$

$$\frac{G - G_m}{G_C - G_m} = \frac{V_C}{1 + (1 - V_C)\dfrac{(G_C - G_m)}{G_m + f_1}} \tag{2b}$$

where

$$f_1 = \frac{G_m(9K_m + 8G_m)}{6(K_m + 2G_m)} \tag{3}$$

Here, the subscripts c and m refer to the ceramic and metal phases, respectively.

The effective Young's modulus E and Poisson's ratio ν can be computed from the following expressions:

$$E = \frac{9KG}{3K + G} \tag{4a}$$

$$\nu = \frac{3K - 2G}{2(3K + G)} \tag{4b}$$

The effective mass density ρ and and length scale parameter l are given by the rule of mixtures as [30 – 34]:

$$\rho(z_{ns}) = (\rho_C - \rho_m)\left(\frac{z_{ns} + z_0}{h} + \frac{1}{2}\right)^k + \rho_m \tag{5a}$$

$$l(z_{ns}) = (l_C - l_m)\left(\frac{z_{ns} + z_0}{h} + \frac{1}{2}\right)^k + l_m \tag{5b}$$

The physical neutral axis of an FG beam can be expressed as function of Láme's constants (λ and μ) by

$$z_0 = \frac{\int_{-h/2}^{h/2} [\lambda(z_{ms}) + 2\mu(z_{ms})] z_{ms} dz_{ms}}{\int_{-h/2}^{h/2} [\lambda(z_{ms}) + 2\mu(z_{ms})] dz_{ms}} \tag{6}$$

It can be noted that distance (z_0) becomes zero for homogeneous beams.

2.1. The modified couple stress theory

Based on the modified couple stress model [10], the strain energy, U , for a linear elastic material occupying region Ω is related to strain and curvature tensors and can be expressed as

$$U = \frac{1}{2}\int_{\Omega} (\sigma_{ij}\varepsilon_{ij} + m_{ij}\chi_{ij}) dV, \quad (i, j = 1,2,3) \tag{7}$$

In which σ , ε , m and χ are Cauchy stress tensor, classical strain tensor, deviatoric part of the couple stress tensor and symmetric curvature tensor, respectively The strain and the curvature tensors are defined by:

$$\varepsilon_{ij} = \frac{1}{2}(u_{i,j} + u_{j,i}) \tag{8a}$$

$$\chi_{ij} = \frac{1}{2}(\theta_{i,j} + \theta_{j,i}) \tag{8b}$$

where u_i are the components of the displacement vector and θ_i hi are the components of the rotation vector given as

$$\theta_i = \frac{1}{2} e_{ijk} u_{k,j} \tag{9}$$

where e_{ijk} is the permutation symbol. The constitutive relations can be written as

$$\sigma_{ij} = \lambda(z_{ns})\varepsilon_{kk}\delta_{ij} + 2\mu(z_{ns})\varepsilon_{ij} \tag{10a}$$

$$m_{ij} = 2\mu(z_{ns})[l(z_{ns})]^2 \chi_{ij} \tag{10b}$$

where δ_{ij} is the Kronecker delta, l is the material length scale parameter which reflects the effect of couple stress, λ and μ are Láme's constants given by

$$\lambda(z_{ns}) = \frac{E(z_{ns})\nu(z_{ns})}{[1+\nu(z_{ns})][1-2\nu(z_{ns})]} \quad \text{and} \quad \mu(z_{ns}) = \frac{E(z_{ns})}{2[1+\nu(z_{ns})]} \tag{11}$$

Based on the same formulation presented by Ould Larbi et al [23] where the transverse displacement is divided with two components (the bending part w_b and the shear part w_s), the axial displacement, u_x, and the transverse displacement of any point of the beam, u_z, are given as

$$u_x(x, z_{ns}, t) = u_0(x,t) - z_{ns}\frac{\partial w_b}{\partial x} - f(z_{ns})\frac{\partial w_s}{\partial x} \tag{12a}$$

$$u_y(x, z_{ns}, t) = 0 \tag{12b}$$

$$u_z(x, z_{ns}, t) = w_b(x,t) + w_s(x,t) \tag{12c}$$

where

- For the classical beam theory (CBT)

$$w_s(x,t) = 0 \tag{13a}$$

- For the new first beam theory (NFBT)

$$f(z_{ns}) = 0 \tag{13b}$$

- For the new sinusoidal beam theory (NSBT)

$$f(z_{ns}) = (z_{ns} + z_0) - \frac{h}{\pi}\sin\frac{\pi(z_{ns}+z_0)}{h} \tag{13c}$$

By using Eq. (8a) and Eqs. (12), the non-zero strains of the present refined beam theory are obtained as

$$\varepsilon_x = \frac{\partial u_0}{\partial x} - z_{ns}\frac{\partial^2 w_b}{\partial x^2} - f(z_{ns})\frac{\partial^2 w_s}{\partial x^2}, \quad \varepsilon_y = \varepsilon_z = \gamma_{xy} = \gamma_{yz} = 0 \tag{14a}$$

$$\gamma_{xz} = 2\varepsilon_{xz} = g(z_{ns})\frac{\partial w_s}{\partial x} \tag{14b}$$

with, $g(z_{ns}) = 1 - f'(z_{ns})$

In addition, equations (8b) and (12) lead to the following expression:

$$\theta_y = -\frac{\partial w_b}{\partial x} - \frac{1}{2}\psi(z_{ns})\frac{\partial w_s}{\partial x}, \quad \theta_x = \theta_z = 0 \tag{15}$$

with, $\psi(z_{ns}) = 1 + f'(z_{ns})$

Substitution of Eq. (15) into (8b) leads to the following expression for the non-zero components of the symmetric curvature tensor

$$\chi_{xy} = -\frac{1}{2}\frac{\partial^2 w_b}{\partial x^2} - \frac{1}{4}\psi(z_{ns})\frac{\partial^2 w_s}{\partial x^2}, \quad \chi_{yz} = -\frac{1}{4}f''(z_{ns})\frac{\partial w_s}{\partial x}, \quad \chi_{xx} = \chi_{yy} = \chi_{zz} = \chi_{xz} = 0 \tag{16}$$

2.2. The governing equations

Hamilton's principle is used in this work to derive the equations of motion. The principle can be stated in analytical form as

$$\int_0^T (\delta U + \delta V - \delta K)dt = 0 \tag{17}$$

where δU is the virtual variation of the strain energy; δV is the virtual variation of the work done by the external applied forces; and δK is the virtual variation of the kinetic energy. The variation of the strain energy of the beam can be stated as

$$\begin{aligned}\delta U &= \int_0^L \int_{-\frac{h}{2}-z_0}^{\frac{h}{2}-z_0} (\sigma_{ij}\delta\varepsilon_{ij} + m_{ij}\delta\chi_{ij})dz_{ns}dx = \int_0^L \int_{-\frac{h}{2}-z_0}^{\frac{h}{2}-z_0} (\sigma_x\delta\varepsilon_x + \tau_{xz}\delta\gamma_{xz} + 2m_{xy}\delta\chi_{xy} + 2m_{yz}\delta\chi_{yz})dz_{ns}dx \\ &= \int_0^L \left(N\frac{d\delta u_0}{dx} - (M_b + Y_1)\frac{d^2\delta w_b}{dx^2} - \left(M_s + \frac{1}{2}Y_1 + \frac{1}{2}Y_2\right)\frac{d^2\delta w_s}{dx^2} + \left(Q - \frac{1}{2}Y_3\right)\frac{d\delta w_s}{dx}\right)dx\end{aligned} \tag{18}$$

where L is the length of the micro-scale beam and the following stress resultants are expressed as

$$(N, M_b, M_s) = \int_{-\frac{h}{2}-z_0}^{\frac{h}{2}-z_0} (1, z_{ns}, f)\,\sigma_x dz_{ns}, \quad Q = \int_{-\frac{h}{2}-z_0}^{\frac{h}{2}-z_0} g\tau_{xz}dz_{ns}, \tag{19a}$$

$$(Y_1, Y_2) = \int_{-\frac{h}{2}-z_0}^{\frac{h}{2}-z_0} (1, f')\, m_{xy}dz_{ns} \quad \text{and} \quad Y_3 = \int_{-\frac{h}{2}-z_0}^{\frac{h}{2}-z_0} f''m_{yz}dz_{ns} \tag{19b}$$

The variation of work done by the external applied forces can be expressed as

$$\delta V = -\int_0^L q\delta(w_b + w_s)dx \tag{20}$$

where q is the transverse load.

The variation of kinetic energy is expressed as

$$\begin{aligned}\delta K &= \int_0^L \int_{-\frac{h}{2}-z_0}^{\frac{h}{2}-z_0} \rho(z_{ns})\left[\dot{u}_x\delta\dot{u}_x + \dot{u}_y\delta\dot{u}_y\right]dz_{ns}dx \\ &= \int_0^L \left\{ I_0\left[\dot{u}_0\delta\dot{u}_0 + (\dot{w}_b + \dot{w}_s)(\delta\dot{w}_b + \delta\dot{w}_s)\right] - I_1\left(\dot{u}_0\frac{d\delta\dot{w}_b}{dx} + \frac{d\dot{w}_b}{dx}\delta\dot{u}_0\right)\right. \\ &\quad + I_2\left(\frac{d\dot{w}_b}{dx}\frac{d\delta\dot{w}_b}{dx}\right) - J_1\left(\dot{u}_0\frac{d\delta\dot{w}_s}{dx} + \frac{d\dot{w}_s}{dx}\delta\dot{u}_0\right) + K_2\left(\frac{d\dot{w}_s}{dx}\frac{d\delta\dot{w}_s}{dx}\right) \\ &\quad \left. + J_2\left(\frac{d\dot{w}_b}{dx}\frac{d\delta\dot{w}_s}{dx} + \frac{d\dot{w}_s}{dx}\frac{d\delta\dot{w}_b}{dx}\right)\right\}dx\end{aligned} \tag{21}$$

where dot-superscript convention indicates the differentiation with respect to the time variable t; $\rho(z_{ns})$ is the mass density; and (I_0, I_1, J_1, I_2, J_2, K_2) are the mass inertias defined as

$$\left(I_0, I_1, J_1, I_2, J_2, K_2\right) = \int_{-\frac{h}{2}-z_0}^{\frac{h}{2}-z_0} \left(1, z_{ns}, f, z_{ns}^2, z_{ns} f, f^2\right) \rho(z_{ns}) dz_{ns} \tag{22}$$

Substituting the expressions for δU, δV, and δK from Eqs. (18), (20), and (21) into Eq.(17) and integrating by parts versus both space and time variables, and collecting the coefficients of δu_0, δw_b, and δw_s, the following equations of motion of the FG micro beam are obtained

$$\delta u_0: \ \frac{dN}{dx} = I_0 \ddot{u}_0 - I_1 \frac{d\ddot{w}_b}{dx} - J_1 \frac{d\ddot{w}_s}{dx} \tag{23a}$$

$$\delta w_b: \ \frac{d^2 M_b}{dx^2} + \frac{d^2 Y_1}{dx^2} + q = I_0(\ddot{w}_b + \ddot{w}_s) + I_1 \frac{d\ddot{u}_0}{dx} - I_2 \frac{d^2 \ddot{w}_b}{dx^2} - J_2 \frac{d^2 \ddot{w}_s}{dx^2} \tag{23b}$$

$$\delta w_s: \ \frac{d^2 M_s}{dx^2} + \frac{1}{2}\frac{d^2 Y_1}{dx^2} + \frac{1}{2}\frac{d^2 Y_2}{dx^2} - \frac{1}{2}\frac{dY_3}{dx} + \frac{dQ}{dx} + q = I_0(\ddot{w}_b + \ddot{w}_s) + J_1 \frac{d\ddot{u}_0}{dx} - J_2 \frac{d^2 \ddot{w}_b}{dx^2} - K_2 \frac{d^2 \ddot{w}_s}{dx^2} \tag{23c}$$

and the following boundary conditions are obtained at $x = 0$ and $x = L$

$$\text{specify } u_0 \text{ or } N \tag{24a}$$

$$\text{specify } w_b \text{ or } V_b \equiv \frac{dM_b}{dx} + \frac{dY_1}{dx} - I_1 \ddot{u}_0 + I_2 \frac{d\ddot{w}_b}{dx} + J_2 \frac{d\ddot{w}_s}{dx} \tag{24b}$$

$$\text{specify } w_s \text{ or } V_s \equiv \frac{dM_s}{dx} + \frac{1}{2}\frac{dY_1}{dx} + \frac{1}{2}\frac{dY_2}{dx} - \frac{1}{2} Y_3 + Q - J_1 \ddot{u}_0 + J_2 \frac{d\ddot{w}_b}{dx} + K_2 \frac{d\ddot{w}_s}{dx} \tag{24c}$$

$$\text{specify } \frac{dw_b}{dx} \text{ or } M_b + Y_1 \tag{24d}$$

$$\text{specify } \frac{dw_s}{dx} \text{ or } M_s + \frac{1}{2} Y_1 + \frac{1}{2} Y_2 \tag{24e}$$

By employing Eqs. (19) and (23), the equations of motion of FG micro beam in terms of the displacements are obtained as

$$A_{11} \frac{d^2 u_0}{dx^2} - B_{11}^s \frac{d^3 w_s}{dx^3} = I_0 \ddot{u}_0 - I_1 \frac{d\ddot{w}_b}{dx} - J_1 \frac{d\ddot{w}_s}{dx} \tag{25a}$$

$$-\left(D_{11} + A_{13}\right) \frac{d^4 w_b}{dx^4} - \left(D_{11}^s + \frac{1}{2}\left(A_{13} + B_{13}\right)\right) \frac{d^4 w_s}{dx^4} + q = I_0(\ddot{w}_b + \ddot{w}_s) + I_1 \frac{d\ddot{u}_0}{dx} - I_2 \frac{d^2 \ddot{w}_b}{dx^2} - J_2 \frac{d^2 \ddot{w}_s}{dx^2} \tag{25b}$$

$$B_{11}^s \frac{d^3 u_0}{dx^3} - \left(D_{11}^s + \frac{1}{2}\left(A_{13} + B_{13}\right)\right) \frac{d^4 w_b}{dx^4} - \left(H_{11}^s + \frac{1}{4}\left(A_{13} + 2B_{13} + D_{13}\right)\right) \frac{d^4 w_s}{dx^4} + \left(A_{55}^s + \frac{1}{4} E_{13}\right) \frac{d^2 w_s}{dx^2} + q = I_0(\ddot{w}_b + \ddot{w}_s) + J_1 \frac{d\ddot{u}_0}{dx} - J_2 \frac{d^2 \ddot{w}_b}{dx^2} - K_2 \frac{d^2 \ddot{w}_s}{dx^2} \tag{25c}$$

where A_{11}, D_{11}, etc., are the beam stiffness, defined by

$$\left(A_{11}, D_{11}, B_{11}^s, D_{11}^s, H_{11}^s\right) = \int_{-\frac{h}{2}-z_0}^{\frac{h}{2}-z_0} \lambda(z_{ns}) \frac{1-\nu(z_{ns})}{\nu(z_{ns})} \left(1, z_{ns}^2, f, z_{ns} f, f^2\right) dz_{ns} \tag{26a}$$

$$\left[A_{13}, B_{13}, D_{13}, E_{13}\right] = \int_{-\frac{h}{2}-z_0}^{\frac{h}{2}-z_0} \mu(z_{ns})\left[l(z_{ns})\right]^2 \left[1, f', (f')^2, (f'')^2\right] dz_{ns} \tag{26b}$$

$$A_{55}^s = \int_{-\frac{h}{2}-z_0}^{\frac{h}{2}-z_0} \mu(z_{ns}) g^2 dz_{ns} \tag{26c}$$

3. Analytical solution

In this work, the Navier solution method for a simply-supported microbeam is adopted to determine the analytical solution. Thus, the following expansions of displacements (u_0, w_b, w_s) are assumed as:

$$\begin{Bmatrix} u_0 \\ w_b \\ w_s \end{Bmatrix} = \sum_{n=1}^{\infty} \begin{Bmatrix} U_n \cos(\lambda x) e^{i\omega t} \\ W_{bn} \sin(\lambda x) e^{i\omega t} \\ W_{sn} \sin(\lambda x) e^{i\omega t} \end{Bmatrix} \tag{27}$$

where U_n, W_{bn}, and W_{sn} are arbitrary parameters to be determined, ω is the eigenfrequency associated with nth eigenmode, and $\lambda = n\pi / L$. The transverse load q is also expanded in Fourier series as

$$q(x) = \sum_{n=1}^{\infty} Q_n \sin(\lambda x) \tag{28}$$

where Q_n is the load amplitude calculated from

$$Q_n = \frac{2}{L} \int_0^L q(x) \sin(\lambda x) dx \tag{29}$$

The coefficient Q_n are given below for some typical loads

$Q_n = q_0$, $n = 1$ for sinusoidal load, (30a)

$$Q_n = \frac{4q_0}{n\pi}, \quad n = 1,3,5..... \text{ for uniform load,} \tag{30b}$$

$$Q_n = \frac{2P}{L} \sin\frac{n\pi}{2}, \quad n = 1,2,3.... \text{ for point load } P \text{ at the midspan,} \tag{30c}$$

Substituting the expansions of u_0, w_b, w_s and q from Eqs (27) and (28) into the equations of motion Eq (25), the analytical solutions can be determined from the following equations:

$$\left(\begin{bmatrix} s_{11} & 0 & s_{13} \\ 0 & s_{22} & s_{23} \\ s_{13} & s_{23} & s_{33} \end{bmatrix} - \omega^2 \begin{bmatrix} m_{11} & m_{12} & m_{13} \\ m_{12} & m_{22} & m_{23} \\ m_{13} & m_{23} & m_{33} \end{bmatrix}\right) \begin{Bmatrix} U_n \\ W_{bn} \\ W_{sn} \end{Bmatrix} = \begin{Bmatrix} 0 \\ Q_n \\ Q_n \end{Bmatrix} \tag{31}$$

where

$$s_{11} = A_{11}\lambda^2,\ \ s_{13} = -B_{11}^s\lambda^3,\ \ s_{22} = \left(D_{11} + A_{13}\right)\lambda^4,\ s_{23} = \left(D_{11}^s + \frac{1}{2}(A_{13} + B_{13})\right)\lambda^4,$$
$$s_{33} = \left(H_{11}^s + \frac{1}{2}\left(B_{13} + \frac{1}{2}\left(D_{13} + A_{13}\right)\right)\right)\lambda^4 + \left(A_{55}^s + \frac{1}{4}E_{13}\right)\lambda^2,$$
$$m_{11} = I_0\,,\ \ m_{12} = -I_1\lambda\,,\ \ m_{13} = -J_1\lambda\,,$$
$$m_{22} = I_0 + I_2\lambda^2\,,\ \ m_{23} = I_0 + J_2\lambda^2\,,\ \ m_{33} = I_0 + K_2\lambda^2\,, \tag{32}$$

Moreover, substituting Eqs (14) into Eq (10a) with the use of Eq (27), one can determine the stress components in terms of Láme's constants and the arbitrary parameters U_n, W_{bn}, and W_{sn} as follows:

$$\sigma_x = \left[\lambda(z_{ns}) + 2\mu(z_{ns})\right]\sum_{n=1}^{\infty}\left\{-\lambda U_n + \lambda^2 W_{bn} z_{ns} + \lambda^2 W_{sn} f(z_{ns})\right\}\sin(\lambda\, x) \tag{33a}$$

$$\tau_{xz} = \mu(z_{ns})g(z_{ns})\sum_{n=1}^{\infty}\lambda W_{sn}\cos(\lambda\, x) \tag{33b}$$

4. Numerical results

In the numerical results, static bending and free vibration of FG microbeams are presented based on the modified couple stress theory and neutral surface-based formulation. The FG microbeams are composed of metal (Al: E_m = 70 GPa, ρ_m = 2702 kg/m^3, ν_m = 0.3) and ceramic (SiC: E_c = 427 GPa, ρ_c = 3100 kg/m^3, ν_c = 0.17) [35].

In the literature studies, it is found that the material length scale parameter is predicted experimentally as 17.6 μm for homogeneous epoxy beam by Lam et al. [9]. Ke and Wang [17] assumed a constant value of 15 μm for functionally graded materials. In this work, we take the length scale parameter of the metallic component l_m as 15 μm. In a number of parametric examples l_c value is taken as 22.5 μm; and in the other cases the ratio l_c / l_m is changed so as to show the effect of the variation of the length scale parameter. The shear correction factor required in the present first shear deformation beam theory is specified as 5/6. The computed values for the bending analysis are obtained by employing 100 terms in series in Eqs. (27) and (28). The employed non-dimensional quantities are:

- Non-dimensional transverse deflection:

$$\bar{w} = 100w\frac{E_m I}{PL^3} \quad \text{for point load}$$

$$\bar{w} = 100w\frac{E_m I}{q_0 L^4} \quad \text{for uniform load}$$

- Non-dimensional stresses:
  - $(\bar{\sigma}_x, \bar{\tau}_{xz}) = \left(\frac{\sigma_x A}{P}, \frac{\tau_{xz} A}{P} \right)$ for point load
- Non-dimensional frequency:

$$\bar{\omega} = \frac{\omega L^2}{h} \sqrt{\frac{\rho_m}{E_m}}$$

4.1 Validation of the results

In order to check the validity and the accuracy of the aforementioned formulations, comparison studies for static and free vibration behaviors using the present theory, have been performed out with the results of the available published works.

4.1.1 Example 1: Bending of a homogeneous micro-beam

The first example is performed for the bending of a homogeneous micro-beam. In Fig. 2, the variation of the transversal displacement and the rotation as against to the normalized beam length is presented and the results are compared with those of Ma et al [13]. The following parameters are employed in calculating the numerical results: $P = 100$ µN, $E = 1.44$ GPa, $\nu = 0.38$, $\rho = 1220$ kg/m^3, $L = 20h$, $b = 2h$, $h = l = 17.6$ µm (where b and h are the width and the thickness of the beam, respectively). From the results plotted in Fig. 2, it can be seen that the results computed via the present theory are in good agreement with those of Ma et al [13].

4.1.2. Example 2: Free vibration of a homogeneous microbeam

The next verification is performed for the natural frequency of the homogeneous microbeam. For this purpose, the variation of the natural frequency is plotted versus the dimensionless material length scale parameter (h/l) in Fig. 3 and the results are compared with those of Ma et al [13]. Again, the computed results are found to be in excellent agreement with those of Ma et al [13].

4.1.3. Example 3: Free vibration of an FG micro-beam

The last example is presented for the dimensionless natural frequencies of FG micro-beam. Indeed, the non-dimensional natural frequencies of FG micro-beam are compared with those of Ansari et al [35] by inserting the material properties used in this reference. Computations in this section are carried out according to the first and sinusoidal shear deformation beam theory in conjunction with the modified couple stress theory and the neutral axis concept. To regenerate the results provided by Ansari et al [35], we set $l_c = l_m = l$ in Eq. (5b). The dimensionless frequencies $\lambda = \omega L \sqrt{I_{00} / A_{110}}$ are employed, where I_{00} and A_{110} are the values I_0 and A_{11} of homogeneous metal micro-beam. In Table 1, the non-dimensional fundamental frequency of FG micro-beam with $k = 2$ is tabulated for different data of the beam thickness. Table 2 presents non-dimensional fifth vibration frequencies of FG micro-beam for various values of the power law index (k) and for $h/l = 2$, $L/h = 10$. The comparisons illustrated in these tables show that the present frequencies are in good agreement with those of the existing literature. However, the small difference between the results computed using the present new sinusoidal beam theory (NSBT) and the first shear deformation beam theories (Timoshenko beam theory [35] and the present NFBT) is due to the use of a constant shear correction factor for any values of power law index k.

4.2. Results for static responses

Tables 3 and 4 tabulate nondimensionalized vertical deflections of the FG micro-beam based on the present unified formulation for various values of the volume fraction exponent k, the ratio l_c/l_m, and two different values of the aspect ratio (L/h= 10, 100). Results are provided for the point load and uniform load. It is seen that the effect of the shear deformation becomes noticeable for the thick micro-beams (i.e., L/h= 10). When l_c/l_m= 1, the length scale parameter of the FG micro-beam is a constant according to Eq. (5b). The same equation also implies that, for the other remaining cases for which $l_c/l_m \neq 1$, the length scale parameter changes within the thickness. Thus, the ratio l_c/l_m indicates the degree of the length scale parameter variation across the beam. It is seen that the increase in the length scale parameter ratio l_c/l_m leads to a decrease of deflection and the results are significantly different to the case where the length scale parameter is assumed to be a constant (l_c/l_m=1). This observation is also a validation of the premise of this work that the variation of the length scale parameter needs to be taken into consideration in the investigation of FG micro-beams. In addition, it is noted as the volume fraction exponent (k) increases, the increase of the deflection will be occur at the same conditions (length scale parameter ratio l_c/l_m, slenderness ratio L/h and loads). In what follows, the results are computed by using the present NSBT. In Fig. 4, the nondimensionalized transverse deflections are presented as a function of the ratio (h/l_m) for different length scale parameter ratio l_c/l_m with considering L/h= 10 and k = 2. It can be seen clearly from Fig. 4 that the vertical deflections predicted by the classical beam model are independent of the material length scale parameter (h/l_m) and they are always larger than those computed using the non-classical beam model with the couple stress. This shows that the introduction of couple stress effect makes a beam stiffer, and hence, leads to a reduction of deflection. However, this effect can be neglected when the material length scale parameter (h/l_m) becomes larger as is shown in Fig. 4. In addition, it can be indicated that as the length scale parameter of the ceramic component gets larger compared to that of the metallic component, the deflection of the FG micro-beam becomes smaller considerably.

Fig. 5 depicts the variation of the nondimensionalized vertical deflections with the volume fraction exponent (k) and the length scale parameter ratio l_c/l_m for two different values of the nondimensionalized material parameter h/l_m and for L/h= 10. It can be seen that the increase of the volume fraction exponent leads to an increase in the vertical deflection. However, the effect of the length scale parameter ratio l_c / l_m on the vertical deflection is not obvious for h / l_m = 8 comparatively to the case where h / l_m = 1. Thus, the sensitivity of the nondimensionalized vertical deflection to the variations in h / l_m becomes rather remarked as this ratio becomes smaller.

In Fig. 6, the variation of the nondimensionalized axial normal stress $\bar{\sigma}_x(L/2, z)$ of the FG micro-beam with L/h = 10 across the thickness is illustrated for different values of the length scale parameter ratio l_c / l_m and for h / l_m = 1 and 8. The axial normal stresses are in compressive state at the top surface of the micro-beam and in tensile state at the bottom side of the beam. Nondimensionalized axial normal stress decreases as the ratio h / l_m is increased from 1/3 to 2. The decrease is much more significant when h / l_m = 1, i.e., the ratio is relatively smaller.

The variation of nondimensionalized transverse stress $\bar{\tau}_{xz}(0, z)$ through the thickness of the FG micro-beam for different values of the length scale parameter ratio l_c / l_m and for h / l_m = 1 and 8, is plotted in Fig. 7. It can be seen that the transverse stress increases as the length scale parameter ratio l_c / l_m decreases. This finding proves also the need to take into consideration the variation of the length scale parameter l across the micro-beam in the analysis of small-scale FG beams.

4.3. Results for free vibration responses

Numerical results on the free vibration behavior of FG micro-beams are given in Table 5 and Figs. 8 and 9. Table 5 lists the dimensionless fundamental frequency corresponding to the transverse deformation mode calculated for various values of the volume fraction exponent (k) and the ratio the length scale parameter ratio (l_c / l_m). It can be seen that the effects of both k and l_c / l_m are significant. For each value of the power law index k, dimensionless frequency decreases considerably as the ratio l_c / l_m is reduced. On the other hand, the decrease in the volume fraction exponent k leads to an increase in the dimensionless frequency. Again, from Table 5 it can be shown the need to consider the change of the length scale parameter l across the micro-beam in the free vibration analysis of small-scale FG beams.

In Fig. 8, both the first and the third nondimensionalized frequency are plotted versus the ratio (h / l_m) for different length scale parameter ratio l_c / l_m with considering L/h = 10 and k = 1. It can be shown clearly from Fig. 8 that the frequency predicted by the classical beam model are independent of the material length scale parameter (h / l_m) and they are always lower than those computed using the non-classical beam model with the couple stress. This shows that the inclusion of couple stress effect makes a beam stiffer, and hence, leads to an increase of frequency. However, this effect can be neglected when the material length scale parameter (h / l_m) becomes larger as is shown in Fig. 8. In addition, it can be indicated that as the length scale parameter of the ceramic component gets larger compared to that of the metallic component, the fundamental frequency of the FG micro-beam becomes larger considerably.

Fig. 9 presents the variation of the nondimensionalized first frequency against the volume fraction exponent (k) and the length scale parameter ratio l_c / l_m for two different values of the nondimensionalized material parameter h / l_m and for $L / h = 10$. It can be shown that the increase of the volume fraction exponent leads to a decrease in the frequency, but for $k \geq 5$ all of the curves become flatter. However, the sensitivity of the nondimensional frequency to the variations in l_c / l_m becomes rather pronounced when the ratio h / l_m gets smaller e.g., $h / l_m = 1$ as is shown in Fig. 9a. The extensive literature on the topic in now available and we can only mention a few recent interesting investigations in refs. [36 – 40].

5. Conclusions

This project presents a novel size-dependent unified beam formulation based on the modified couple stress theory for the bending and free vibration responses of FG micro-beams, that consider a variable length scale parameter. In this formulation, the vertical displacement is decomposed into both bending and shear components in such a way that, the proposed approach make it easy to provide results regarding three different beam models, which are classical beam theory (CBT), new first beam theory (NFBT), and new sinusoidal beam theory (NSBT). Mori–Tanaka homogenization method is employed to predict the material properties of the FG micro-beam. Hamilton's principle in conjunction with the neutral surface concept is employed to determine the equations of motion. The results obtained using the present size-dependent unified neutral surface-based beam formulation, are compared with the existing theoretical results to prove the validity of the present approach. This work justifies also the development of a general approach for the analysis of FG micro-beams having a variable length scale parameter. It was confirmed that the parameter showing the degree of length scale parameter variation, i.e. l_c / l_m, considerably affects both the bending and the free vibration behaviors of a FG micro-beam. In addition, the findings of this work showed that the inclusion of couple stress effect makes a micro-beam stiffer, and hence, leads to a reduction of the vertical displacement and an increase of frequency. This fact proves the insufficient precision of classical theory in predicting the mechanical response of micro-beams and shows the need of employing non-classical theories.

Acknowledgement

This project was funded by the Deanship of Scientific Research (DSR), King Abdulaziz University, Jeddah, under grant No. (130 - 282 - D1435). The authors, therefore, acknowledge with thanks DSR technical and financial support. The authors are also thankful to Dr. Abdelhakim Kaci from Material and Hydrology Laboratory, for his support.

References

1. Fu Y, Du H, Zhang S. Functionally graded TiN/TiNi shape memory alloy films. Mater Lett 2003;57:2995–9.
2. Witvrouw A, Mehta A. The use of functionally graded Ploy-SiGe Layers for MEMS Applications. Mater Sci Forum 2005;492–493:255–60.
3. Lü CF, Lim CW, Chen WQ. Size-dependent elastic behavior of FGM ultra-thin films based on generalized refined theory. Int J Solids Struct 2009;46:1176–85.
4. Hasanyan DJ, Batra RC, Harutyunyan S. Pull-in instabilities in functionally graded microthermoelectromechanical systems. J Therm Stresses 2008;31:1006–21.
5. Mohammadi-Alasti B, Rezazadeh G, Borgheei AM, Minaei S, Habibifar R. On the mechanical behavior of a functionally graded micro-beam subjected to a thermal moment and nonlinear electrostatic pressure. Compos Struct 2011;93:1516–25.
6. Zhang J, Fu Y. Pull-in analysis of electrically actuated viscoelastic microbeams based on a modified couple stress theory. Meccanica 2012; 47: 1649 – 1658.
7. Rahaeifard M, Kahrobaiyan MH, Ahmadian MT. Sensitivity analysis of atomic force microscope cantilever made of functionally graded materials. In: DETC2009-86254, 3rd international conference on micro- and nanosystems (MNS3) 2009, San Diego, CA, USA; 2009.
8. Toupin RA. Elastic materials with couple stresses. Arch Ration Mech Anal 1962;11:385–414.
9. Lam DCC, Yang F, Chong ACM, Wang J, Tong P. Experiments and theory in strain gradient elasticity. J Mech Phys Solids 2003;51:1477–508.
10. Yang F, Chong ACM, Lam DCC, Tong P. Couple stress based strain gradient theory for elasticity. Int J Solids Struct 2002; 39: 2731–43.
11. Park SK, Gao XL. Bernoulli–Euler beam model based on a modified couple stress theory. Journal of Micromechanics and Microengineering 2006;16:2355–9.
12. Kong SL, Zhou SJ, Nie ZF, Wang K. The size-dependent natural frequency of Bernoulli–Euler micro-beams. International Journal of Engineering Science 2008;46(5):427–37.
13. Ma HM, Gao XL, Reddy JN. A microstructure-dependent Timoshenko beam model based on a modified couple stress theory. Journal of Mechanics and Physics of Solids 2008;56(12):3379–91.
14. Ma HM, Gao XL, Reddy JN. A nonclassical Reddy–Levinson beam model based on a modified couple stress theory. Journal for Multiscale Computational Engineering 2010;8(2):167–80.
15. Asghari M, Ahmadian MT, Kahrobaiyan MH, Rahaeifard M. On the size- dependent behavior of functionally graded micro-beams. Materials & Design 2010;31:2324–9.
16. Asghari M, Kahrobaiyan MH, Rahaeifard M, Ahmadian MT. The modified couple stress functionally graded Timoshenko beam formulation. Materials & Design 2011;32:1435–43.

17. Ke LL, Wang YS. Size effect on dynamic stability of functionally graded microbeams based on a modified couple stress theory. Composite Structures 2011;93:342–50.
18. Nateghi A, Salamat-talab M, Rezapour J, Daneshian B. Size Dependent BucklingAnalysis of Functionally Graded Micro Beams Based on Modified Couple Stress Theory. Applied Mathematical Modelling 2012; 36: 4971 – 4987.
19. Reddy JN. Microstructure-dependent couple stress theories of functionally graded beams. Journal of the Mechanics and Physics of Solids 2011;59:2382–99.
20. Kahrobaiyan, M.H., Rahaeifard, M., Tajalli, S.A., Ahmadian, M.T. “A strain gradient functionally graded EulereBernoulli beam formulation”, Int. J. Eng. Sci. (2012) 52, 65 – 76.
21. Yahoobi H., Feraidoon A. Influence of neutral surface position on deflection of functionally graded beam under uniformly distributed load. World Appl. Sci. J. 2010; 10(3): 337-341.
22. Bouremana M., Houari M.S.A., Tounsi A, Kaci A., Adda Bedia E.A. A new first shear deformation beam theory based on neutral surface position for functionally graded beams. Steel and Composite Structures 2013; 15(5): 467-479.
23. Ould Larbi L, Kaci A., Houari M.S.A., Tounsi A. An efficient shear deformation beam theory based on neutral surface position for bending and free vibration of functionally graded beams. Mechanics Based Design of Structures and Machines 2013; 41: 421–433.
24. Fekrar, A., Houari, M.S.A., Tounsi, A., Mahmoud, S.R. (2014), “A new five-unknown refined theory based on neutral surface position for bending analysis of exponential graded plates”, *Meccanica*, **49**, 795 – 810.
25. Bousahla, A.A., Houari, M.S.A., Tounsi, A., Adda Bedia, E.A., (2014), “A novel higher order shear and normal deformation theory based on neutral surface position for bending analysis of advanced composite plates”, *International Journal of Computational Methods*, 11(6), 1350082.
26. Khalfi, Y., Houari, M.S.A., Tounsi, A. (2014), “A refined and simple shear deformation theory for thermal buckling of solar functionally graded plates on elastic foundation”, *International Journal of Computational Methods*, **11(5)**, 135007.
27. Z.-Q. Cheng, R. Batra, Three-dimensional thermoelastic deformations of a functionally graded elliptic plate. Composites Part B: Engineering 2 (2000) 97–106.
28. L. Qian, R. Batra, L. Chen, Static and dynamic deformations of thick functionally graded elastic plates by using higher-order shear and normal deformable plate theory and meshless local Petrov–Galerkin method. Composites Part B: Engineering 35 (2004) 685–697.
29. Belabed, Z., Houari, M.S.A., Tounsi, A., Mahmoud, S.R., Anwar Bég, O. (2014), "An efficient and simple higher order shear and normal deformation theory for functionally graded material (FGM) plates”, *Composites: Part B*, **60**, 274–283.

30. S. Natarajan, P. Baiz, M. Ganapathi, P. Kerfriden, S. Bordas, Linear free flexural vibration of cracked functionally graded plates in thermal environment. Computers and Structures 89 (2011) 1535–1546.
31. Benachour, A., Daouadji Tahar, H., Ait Atmane, H., Tounsi, A., Meftah, S.A. (2011), "A four variable refined plate theory for free vibrations of functionally graded plates with arbitrary gradient", *Composites: Part B*, **42**, 1386-1394.
32. Bessaim, A., Houari, M.S.A., Tounsi, A., Mahmoud, S.R., Adda Bedia, E.A. (2013), "A new higher-order shear and normal deformation theory for the static and free vibration analysis of sandwich plates with functionally graded isotropic face sheets", *Journal of Sandwich Structures and Materials*, **15(6)**, 671 – 703.
33. Tounsi, A., Houari, M.S.A., Benyoucef, S., Adda Bedia, E.A. (2013), "A refined trigonometric shear deformation theory for thermoelastic bending of functionally graded sandwich plates", *Aerospace Science and Technology*, **24**, 209 – 220.
34. Mahi, A., Adda Bedia, E.A., Tounsi, A. (2014), "A new hyperbolic shear deformation theory for bending and free vibration analysis of isotropic, functionally graded, sandwich and laminated composite plates", *Applied Mathematical Modelling*, (In press).
35. Ansari, R., Gholami, R., & Sahmani, S. (2011). Free vibration analysis of size-dependent functionally graded microbeams based on the strain gradient Timoshenko beam theory. Composite Structures, 94, 221–228.
36. S. R. Mahmoud, "On problem of Shear waves in a magneto-elastic half-space of initially stressed a non-homogeneous anisotropic material under influence of rotation", International Journal of Mechanical Sciences, oi.org/10.1016/j.ijmecsci.2013.10.004i, (2013).
37. M. Marin, "The Lagrange identity method in thermoelasticity of bodies with microstructure", Int. J. Engng. Sci., Elsevier, vol. 32, 8, pp.1229-1240; (1994).
38. S. R. Mahmoud , "Effect of non-homogeneity and rotation on an infinite generalized thermoelastic diffusion medium with a spherical cavity subject to magnetic field and initial stress", Abstract and Applied Analysis, Vol. 2013, Article ID 284646, (2013).
39. M. Marin, R. P. Agarwal , S. R. Mahmoud "Nonsimple material problems addressed by the Lagrange's identity", Boundary Value Problems, Vol.2013, 2013 :135, doi. org/10.1186/1687-2770-2013-135, (2013)
40. S. R. Mahmoud, "Analytical solution for free vibrations of elastodynamic orthotropic hollow sphere under the influence of rotation", Journal of Computational and Theoretical Nanoscience, Vol.11,1,pp. 137-146,(2014).

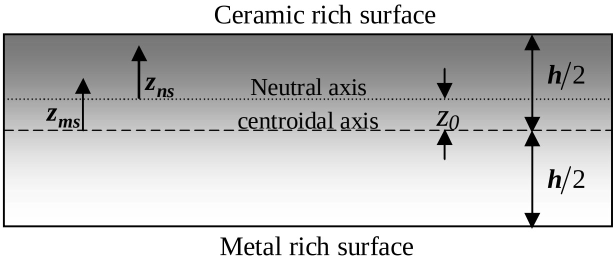

Fig. 1: The position of centroidal axis and neutral axis for a FG beam.

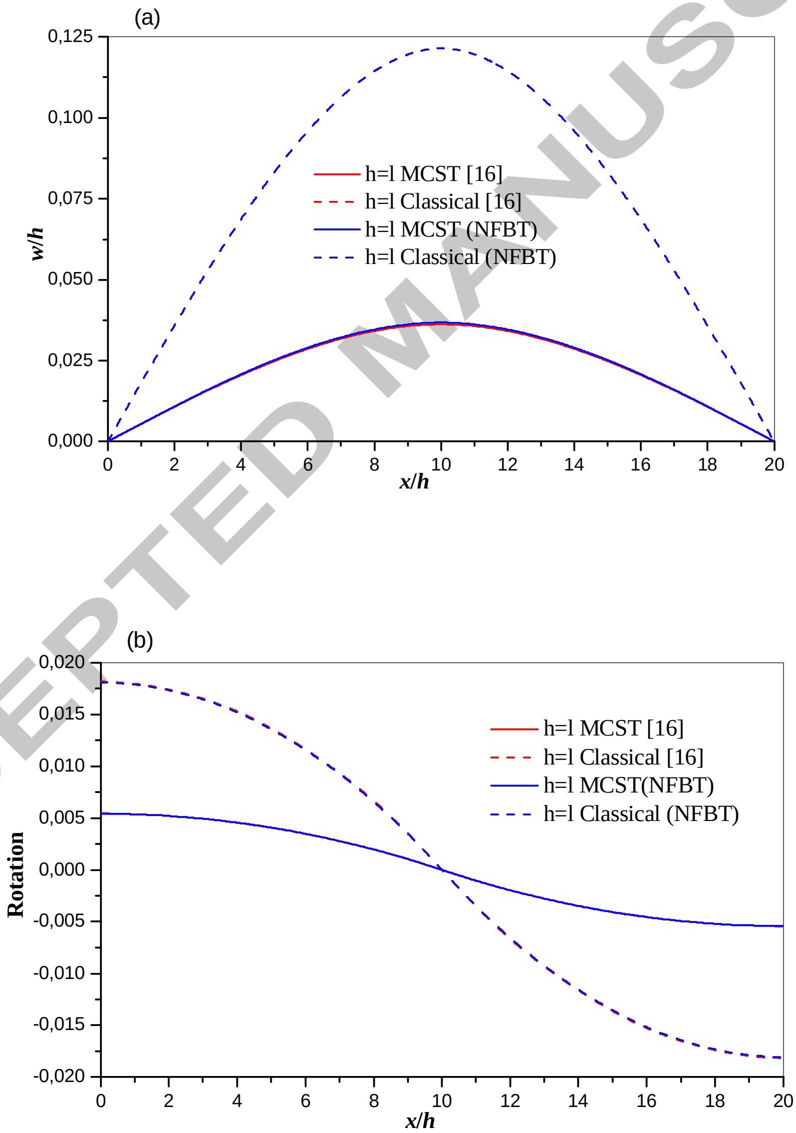

Fig. 2: Comparison of the normalized static deflections and rotations of the simply supported microbeam subjected to a point load at the middle for $P = 100\ \mu\text{N}$, $L = 20h$, $b = 2h$, $\nu = 0.38$.

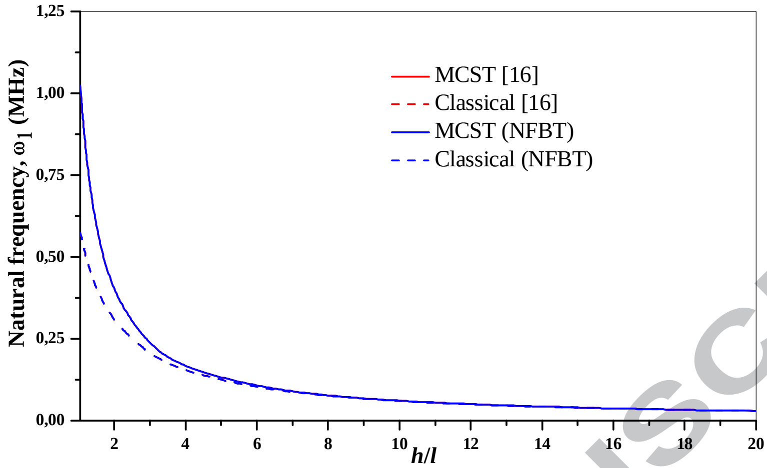

Fig. 3: Comparison of the natural frequency of the simply supported microbeam for $L = 20h$, $b = 2h$, $\nu = 0.38$.

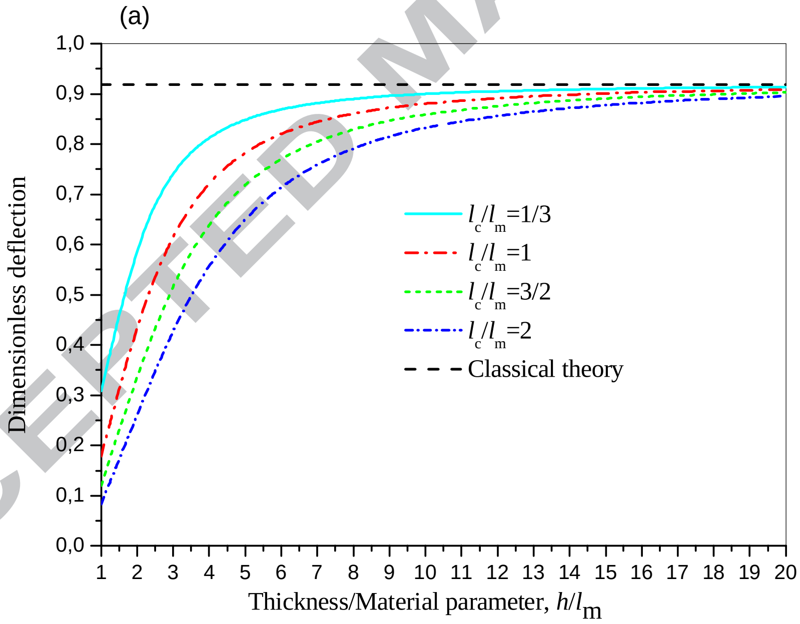

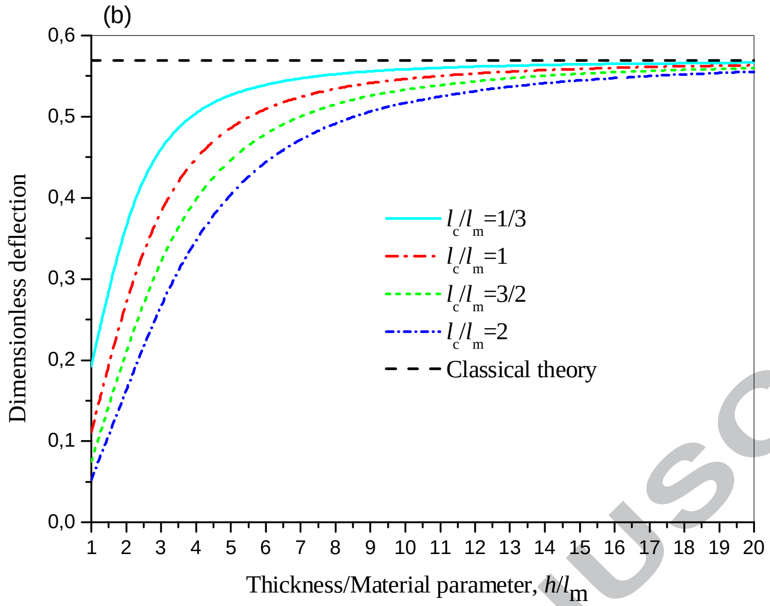

Fig. 4: Variation of the dimensionless transverse deflections of the FG micro-beam for different values of the length scale parameter ratio l_c / l_m, $L / h = 10$, $l_m = 15\mu m$, $b / h = 1$, $k = 2$.(a) point load. (b) uniform load.

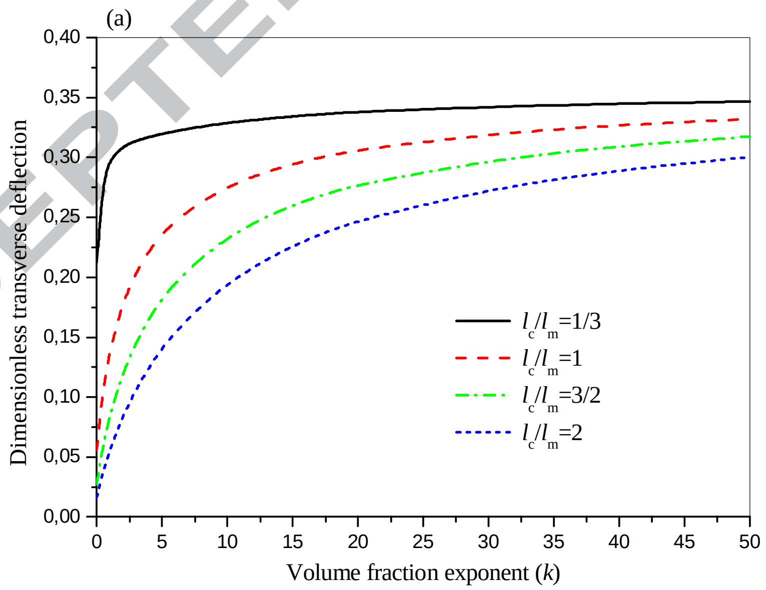

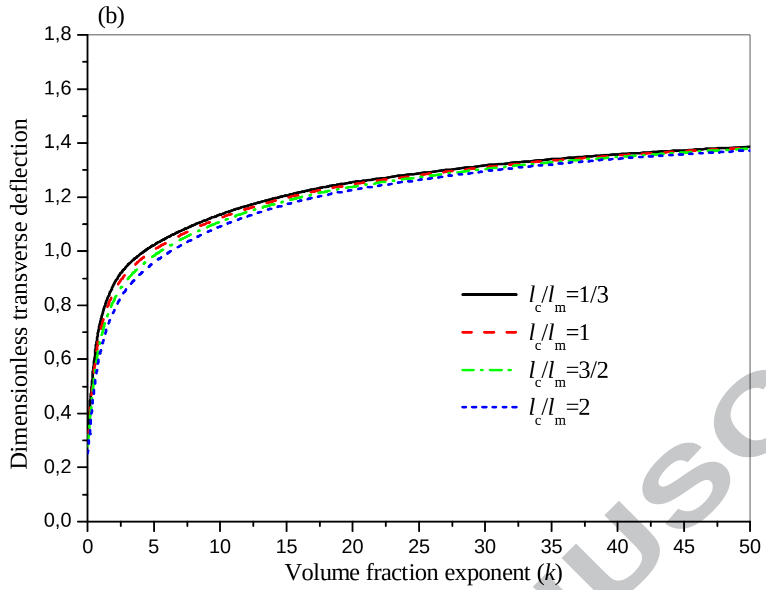

Fig. 5: Variation of the dimensionless transverse deflections of the FG micro-beam subjected to a point load with the volume fraction exponent for, $L/h=10$, $l_m=15\mu m$ (a) $h/l_m=1$, (b) $h/l_m=8$.

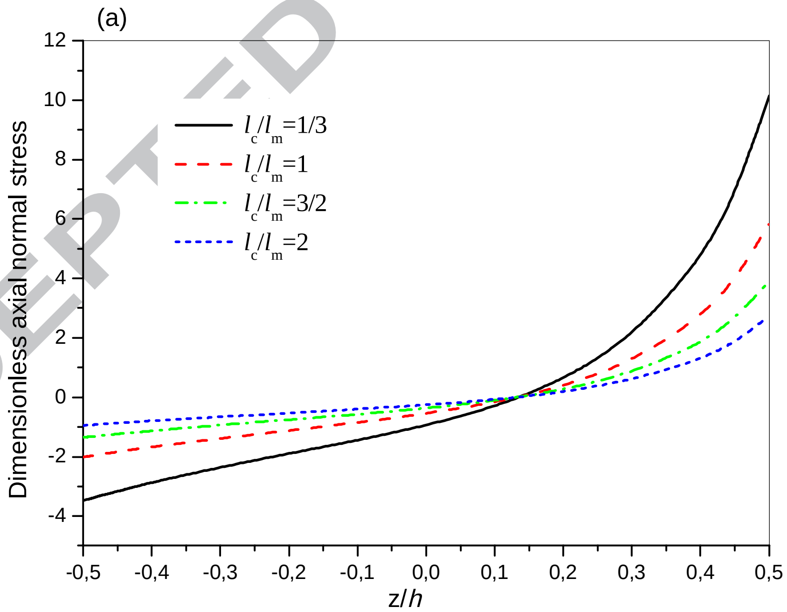

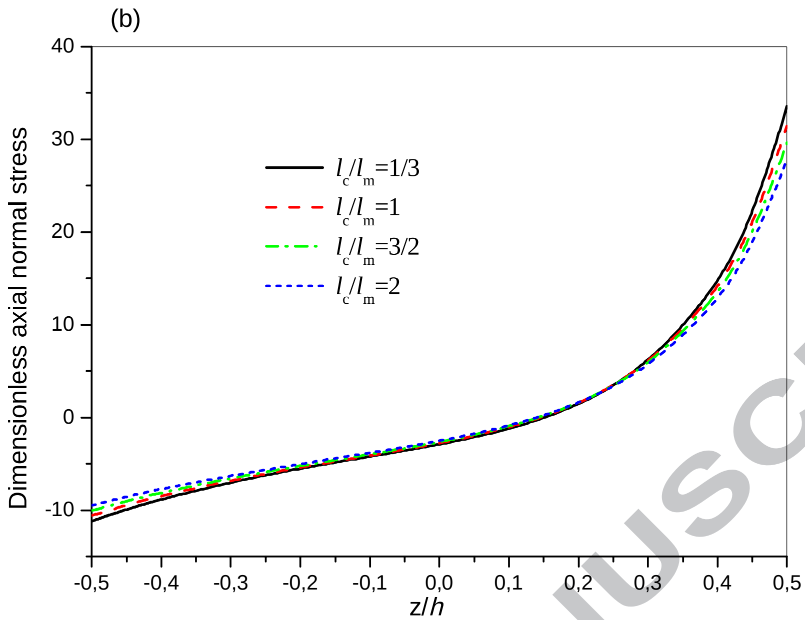

Fig. 6: Variation of the normal stress across the thickness of FG micro-beam subjected to a point load, for different values of the length scale parameter ratio with $L/h=10$, $l_m=15\mu m$, $k=2$, $b=2h$: (a) $h/l_m=1$, (b) $h/l_m=8$.

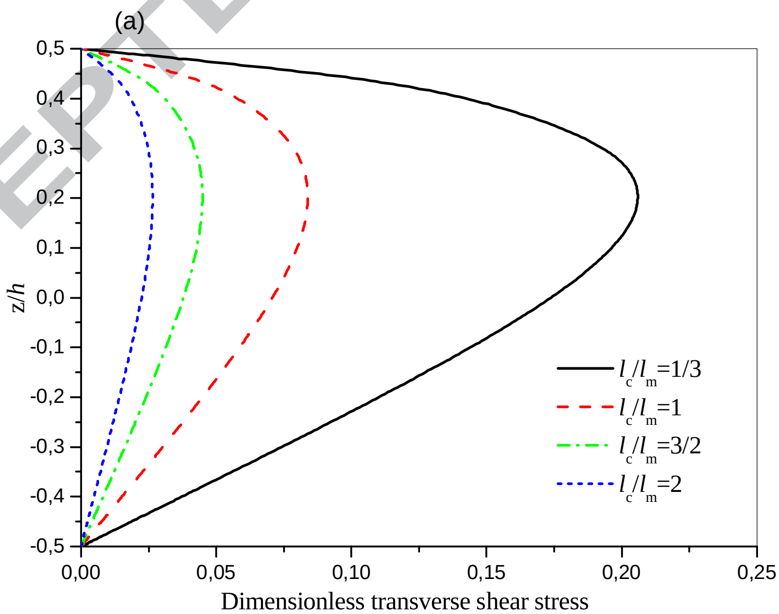

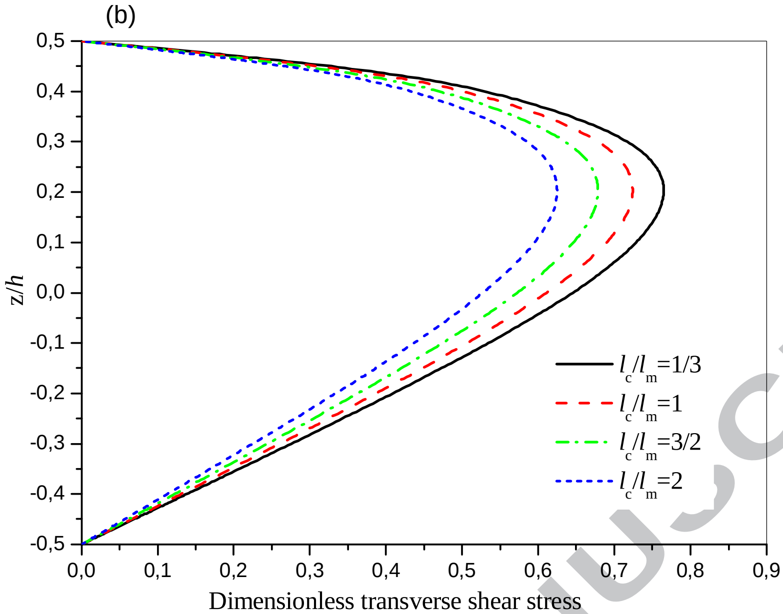

Fig. 7: Variation of the transverse stress across the thickness of FG micro-beam subjected to a point load, for different values of the length scale parameter ratio with $L/h=10$, $l_m=15\mu m$, $k=2$, $b=h$: (a) $h/l_m=1$, (b) $h/l_m=8$.

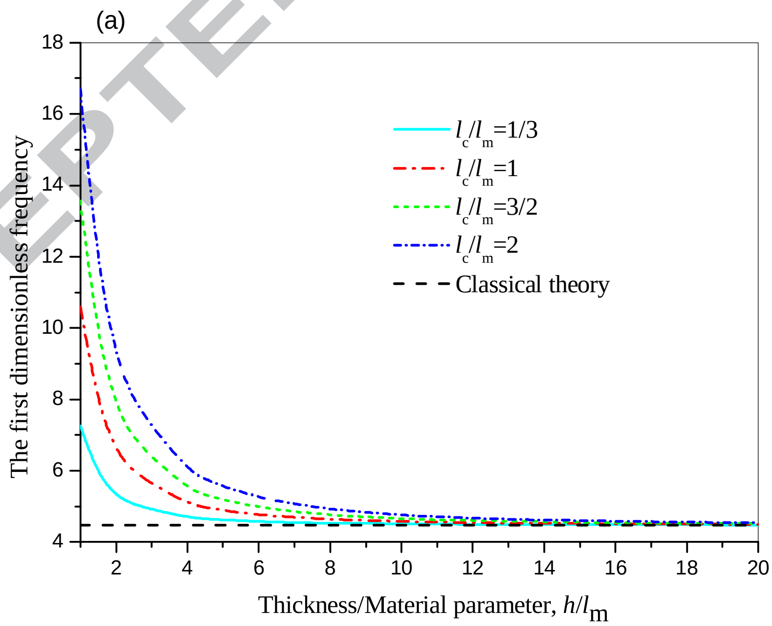

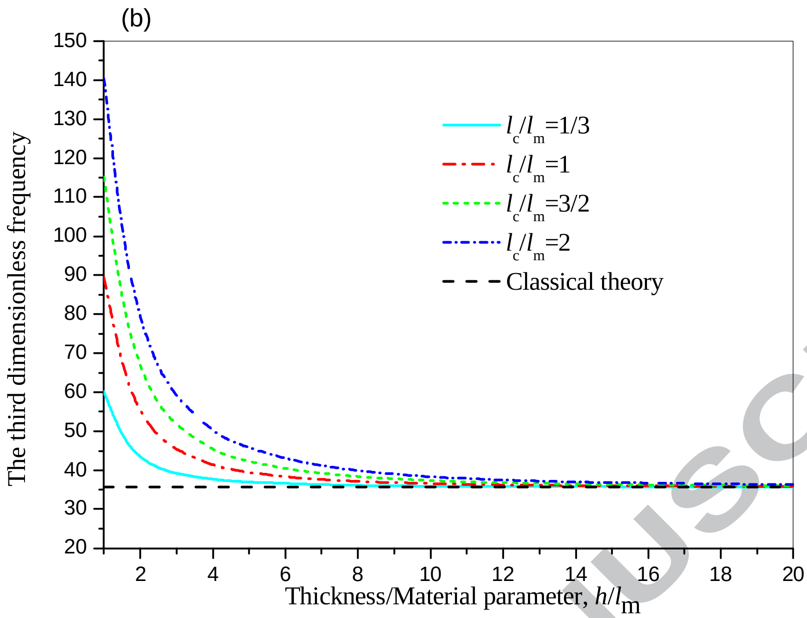

Fig. 8: Variation of the dimensionless frequencies of the FG micro-beam for different values of the length scale parameter ratio l_c / l_m, $L / h = 10$, $l_m = 15\mu m$, $b / h = 1$, $k = 1$.(a) the first frequency. (b) the third frequency.

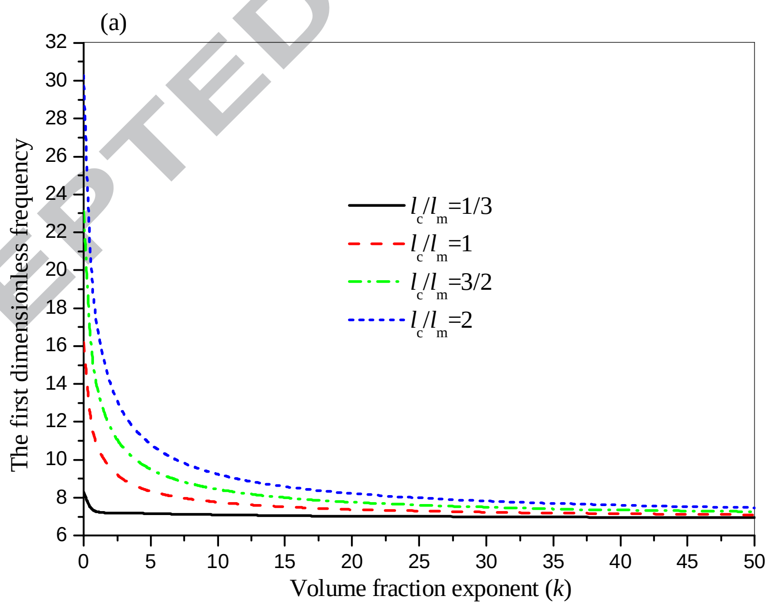

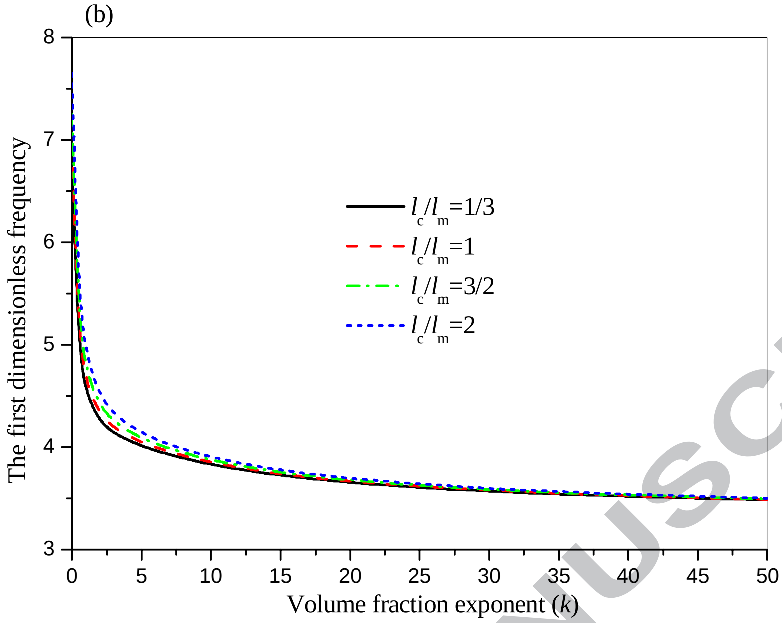

Fig. 9: Variation of the first dimensionless frequencies of the FG micro-beam versus the volume fraction exponent for $L/h = 10$: (a) $h/l_m = 1$. (b) $h/l_m = 8$.

Table 1: Comparison of the dimensionless fundamental frequencies of the FG micro-scale beam with $k = 2$, $L = 10h$ (the first mode, $n = 1$).

h (μm)	15	30	45	60	75	90	120
Present (NSBT)	0.8151	0.5140	0.4357	0.4047	0.3894	0.3809	0.3723
Present (NFBT)	0.7982	0.5099	0.4340	0.4040	0.3893	0.3811	0.3727
Ansari et al [35]	0.7983	0.5100	0.4341	0.4041	0.3894	0.3811	0.3728

Table 2: Comparison of the dimensionless fifth frequencies of the FG micro-scale beam with $h/l = 2$, $L = 10h$ (the fifth mode, $n = 5$).

Model	Ceramic	$k = 0.1$	$k = 0.6$	$k = 1.2$	$k = 2$	$k = 10$	Metal
Present (NSBT)	17.9097	15.9659	12.7215	11.4024	10.5845	8.8607	7.7223
Present (NFBT)	16.4670	14.7264	11.6880	10.3916	9.5585	7.8452	6.9885
Ansari et al [35]	16.4672	14.7194	11.6879	10.3919	9.5590	7.8479	7.0831

Table 3: Dimensionless transverse deflections of the FG micro-beam for point load. $l_m = 15$, $h/l_m = 2$, $b/h = 1$.

l_c/l_m	Beam theory	$L/h = 10$				$L/h = 100$			
		k =0.3	k =1	k =3	k =10	k =0.3	k =1	k =3	k =10
1/3	CBT	0.4225	0.5426	0.6206	0.6939	0.4225	0.5426	0.6206	0.6939
	NFBT	0.4349	0.5599	0.6454	0.7263	0.4227	0.5427	0.6209	0.6942
	NSBT	0.4331	0.5570	0.6403	0.7155	0.4227	0.5427	0.6208	0.6941
1	CBT	0.2394	0.3564	0.4909	0.6302	0.2394	0.3564	0.4910	0.6302
	NFBT	0.2473	0.3690	0.5116	0.6603	0.2395	0.3566	0.4912	0.6305
	NSBT	0.2437	0.3628	0.5011	0.6452	0.2394	0.3565	0.4910	0.6304
3/2	CBT	0.1542	0.2526	0.3959	0.5712	0.1542	0.2526	0.3959	0.5712
	NFBT	0.1605	0.2629	0.4138	0.5993	0.1543	0.2527	0.3961	0.5715
	NSBT	0.1565	0.2560	0.4018	0.5823	0.1542	0.2527	0.3959	0.5713
2	CBT	0.1041	0.1824	0.3163	0.5098	0.1041	0.1824	0.3163	0.5098
	NFBT	0.1094	0.1913	0.3321	0.5358	0.1041	0.1825	0.3165	0.5101
	NSBT	0.1054	0.1844	0.3197	0.5174	0.1041	0.1825	0.3164	0.5099
Classical theory	CBT	0.5313	0.7587	0.9383	1.1245	0.5316	0.7587	0.9383	1.1245
	NFBT	0.5470	0.7828	0.9753	1.1760	0.5315	0.7589	0.9387	1.1250
	NSBT	0.5470	0.7848	0.9826	1.1826	0.5315	0.7590	0.9387	1.1251

Table 4: Dimensionless transverse deflections of the FG micro-beam for uniform load. $l_m = 15$, $h/l_m = 2$, $b/h = 1$.

l_c/l_m	Beam theory	$L/h = 10$				$L/h = 100$			
		k =0.3	k =1	k =3	k =10	k =0.3	k =1	k =3	k =10
1/3	CBT	0.2641	0.3391	0.3879	0.4337	0.2641	0.3391	0.3879	0.4337
	NFBT	0.2704	0.3480	0.4007	0.4505	0.2642	0.3392	0.3880	0.4338
	NSBT	0.2695	0.3465	0.3981	0.4449	0.2641	0.3392	0.3880	0.4338
1	CBT	0.1496	0.2228	0.3069	0.3939	0.1497	0.2228	0.3069	0.3940
	NFBT	0.1538	0.2293	0.3176	0.4095	0.1497	0.2228	0.3069	0.3940
	NSBT	0.1519	0.2261	0.3123	0.4020	0.1497	0.2228	0.3069	0.3940
3/2	CBT	0.0964	0.1579	0.2474	0.3570	0.0964	0.1579	0.2474	0.3570
	NFBT	0.0996	0.1632	0.2568	0.3716	0.0964	0.1579	0.2475	0.3572
	NSBT	0.0975	0.1597	0.2505	0.3628	0.0964	0.1579	0.2475	0.3571
2	CBT	0.0650	0.1140	0.1977	0.3186	0.0650	0.1140	0.1977	0.3186
	NFBT	0.0678	0.1187	0.2059	0.3322	0.0651	0.1141	0.1978	0.3188
	NSBT	0.0657	0.1150	0.1995	0.3226	0.0651	0.1140	0.1977	0.3187
Classical theory	CBT	0.3321	0.4742	0.5864	0.7028	0.3321	0.4742	0.5864	0.7028
	NFBT	0.3399	0.4863	0.6050	0.7286	0.3322	0.4743	0.5866	0.7031
	NSBT	0.3400	0.4874	0.6089	0.7323	0.3322	0.4743	0.5867	0.7031

Table 5: Dimensionless fundamental frequency of the FG microbeam. $l_m = 15$, $h/l_m = 2$, $b/h = 1$.

l_c/l_m	Beam theory	$L/h = 10$				$L/h = 100$			
		k =0.3	k =1	k =3	k =10	k =0.3	k =1	k =3	k =10
1/3	CBT	5.9695	5.3625	5.1021	4.8828	5.9954	5.3878	5.1262	4.9039
	NFBT	5.8987	5.2933	5.0198	4.7902	5.9947	5.3871	5.1253	4.9029
	NSBT	5.9090	5.3043	5.0362	4.8203	5.9948	5.3872	5.1255	4.9033
1	CBT	7.9307	6.6159	5.7362	5.1231	7.9651	6.6471	5.7633	5.1453
	NFBT	7.8233	6.5211	5.6383	5.0237	7.9640	6.6461	5.7623	5.1442
	NSBT	7.8722	6.5670	5.6876	5.0731	7.9645	6.6466	5.7628	5.1448
3/2	CBT	9.8817	7.8588	6.3882	5.3815	9.9246	7.8959	6.4185	5.4048
	NFBT	9.7187	7.7289	6.2710	5.2742	9.9229	7.8945	6.4172	5.4036
	NSBT	9.8225	7.8152	6.3490	5.3384	9.9240	7.8955	6.4181	5.4043
2	CBT	12.0283	9.2477	7.1465	5.6963	12.0805	9.2914	7.1804	5.7209
	NFBT	11.7780	9.0658	7.0021	5.5783	12.0778	9.2894	7.1788	5.7197
	NSBT	11.9658	9.2077	7.1153	5.6611	12.0798	9.2910	7.1801	5.7206
Classical theory	CBT	5.3280	4.5348	4.1494	3.8353	5.3511	4.5561	4.1691	3.8519
	NFBT	5.2654	4.4775	4.0848	3.7661	5.3505	4.5555	4.1684	3.8512
	NSBT	5.2649	4.4723	4.0719	3.7564	5.3504	4.5555	4.1682	3.8511